Supplementary information for the "Indentation response of soft viscoelastic matter with hard skin"

Yanwei Liu, Yueguang Wei* and Pu Chen

Department of Mechanics and Engineering Science, College of Engineering, Peking University, Beijing 100871, China

* Corresponding author: E-mail address: weiyg@pku.edu.cn

1. The detailed derivation for Eqs. (5) and (6)

The Hankel transformation is an expression form of a function, in which the given function is expanded by a series of Bessel function of the first kind. For example, the k-th order Hankel transformation and inverse transformation for f(r) are

$$\overline{f}_k(\xi) = \int_0^\infty f(r) J_k(\xi r) r dr \tag{S1}$$

$$f(r) = \int_0^\infty \overline{f}_k(\xi) J_k(\xi r) \xi d\xi \tag{S2}$$

Based on the above definition, the zero-order Hankel transformation of f(r) can be written as

$$f(r) = \int_0^\infty \overline{f}_0(\xi) J_0(\xi r) \xi d\xi \tag{S3}$$

The first and second derivative of f(r) with respect to r are

$$\frac{df(r)}{dr} = -\int_0^\infty \xi^2 \overline{f}_0(\xi) J_1(\xi r) d\xi \tag{S4}$$

$$\frac{d^2 f(r)}{dr^2} = -\int_0^\infty \xi^3 \overline{f}_0(\xi) [J_0(\xi r) - \frac{J_1(\xi r)}{\xi r}] d\xi \tag{S5}$$

Based on Eqs. (S4) and (S5), $\nabla^2 w(r)$ in Eq.(1) can be expressed as

$$\nabla^2 w(r) = (\frac{\partial^2}{\partial r^2} + \frac{\partial}{r \partial r}) w(r) = -\int_0^\infty \xi^3 \overline{w}(\xi) J_0(\xi r) d\xi \tag{S6}$$

According the definition of Hankel transformation and Eq. (S6) we can get

$$\nabla^2 \overline{w_0}(\xi) = \int_0^\infty \nabla^2 w(r) J_0(\xi r) r dr = -\xi^2 \overline{w_0}(\xi) \tag{S7}$$

Then the Hankel transformation of Eq. (1) can be expressed as

$$D\xi^4 \overline{\omega}(\xi) = \overline{q}(\xi) - \overline{p}(\xi) \tag{S8}$$

The longitudinal displacement of any point in a semi-infinite elastic body under any axisymmetric load can be expressed as

$$w(r,z)=\frac{1+v}{E}\int_0^\infty (2-2v+\xi z)e^{-\xi z}\overline{p}(\xi)J_0(\xi r)d\xi \tag{S9}$$

According to Eq. (S9), the displacement of the surface of the semi-infinite elastic body is

$$w(r,0)=\frac{2(1-v^2)}{E}\int_0^\infty \overline{p}(\xi)J_0(\xi r)d\xi \tag{S10}$$

2. Fig. S1 to Fig.S8

Finite element models were established to verify the our hypothesis about the contact stress distribution. The detailed information about the finite element model can be found in section 3 of the paper.

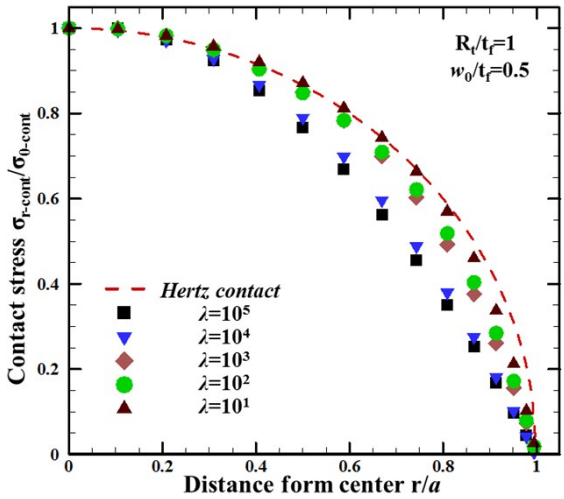

Fig. S1 Contact stress at different modulus ratio of the film to the substrate when the indentation depth, w_0/t_f, is 0.5 and the indenter radius, R_t/t_f, is 1. The different symbols are for FEM results at different λ (modulus ratio of the film to the substrate), and the red dotted line is for Hertz contact stress distribution.

We output the contact stress distribution within the contact radius to verify the rationality of our hypothesis. As shown in Fig. S1, the Hertz distribution can basically describe the contact stress distribution state, which shows that our assumption is reasonable.

To more clearly illustrate the imaginary error function in Eq.(18), its graph is shown in Fig. S2.

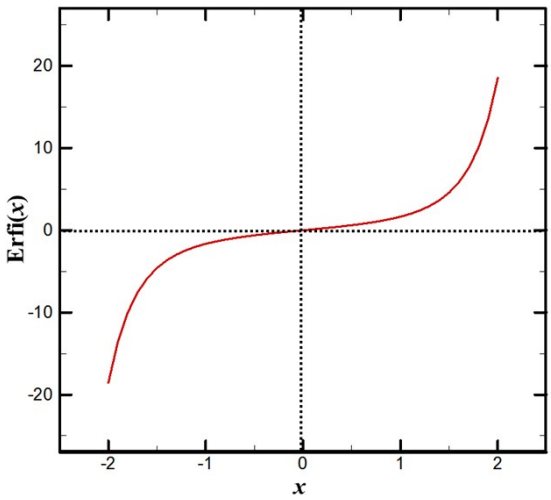

Fig. S2 The graph of the imaginary error function.

In order to prove that the indentation response of the hard film/soft substrate system with high modulus ratio is not sensitive to the size of the indenter, taking the modulus ratio of 10^4 as an example, the relationship between indentation loads and displacements at different indenter radius is shown in Fig. S3. Fig. S3 (a) shows the relationship of load and relaxation time at different indenter radius when the modulus ratio is 10^4. It can be seen from Fig. S3 (a) that when the indenter radius changes from 1 to 3, the maximum error between theory and FEM is no more than 5%. Fig. S3 (b) shows the relationship of load and depth at different indenter radius when the modulus is 10^4. From Fig. S3 (b), we can know that when the indenter radius changes from 1 to 3, the maximum error between the theory and the FEM does not exceed 0.8%.

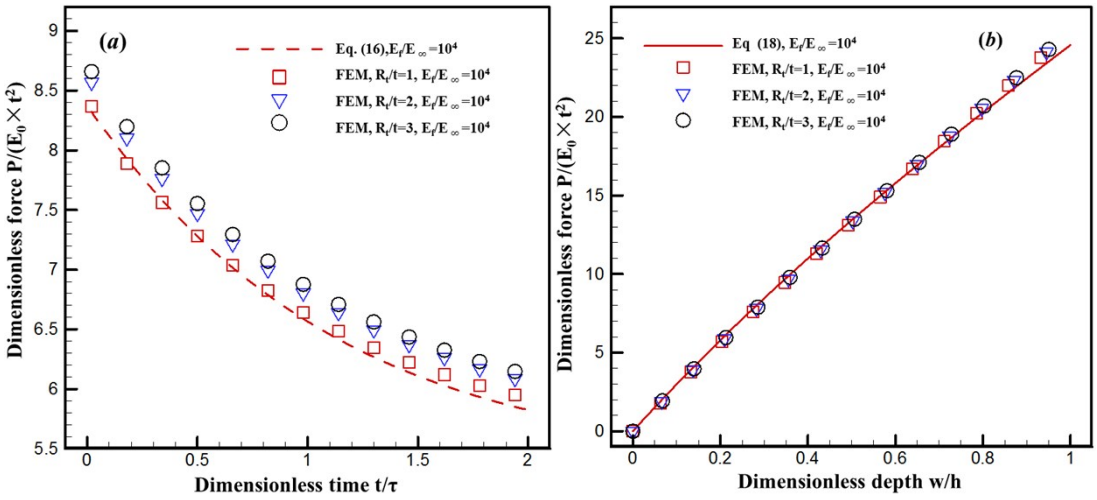

Fig.S3 (a) The relationship of load and relaxation time at different indenter radius when the modulus ratio is 10^4. The red dash line is for Eq.(16), and various symbols are

for FEM results. In those example, the ratio of the decay modulus to the equilibrium modulus, g, takes 1, and the dimensionless indentation depth, w_0/t_f, is 0.25; (b) the relationship of load and depth at different indenter radius when the modulus ratio is 10^4. The red solid line is for Eq.(18), and various symbols are for FEM results. In those example, the ratio of the decay modulus to the equilibrium modulus, g, takes 1, and the dimensionless indentation speed , $v_0\tau/t_f$, is equal to 0.5.

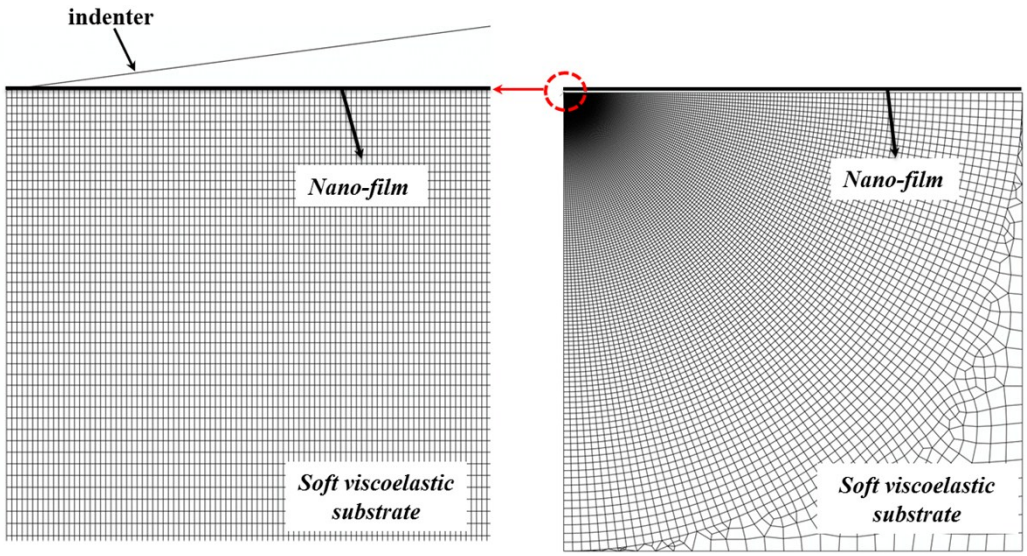

Fig. S4 The finite element meshes used in all simulations

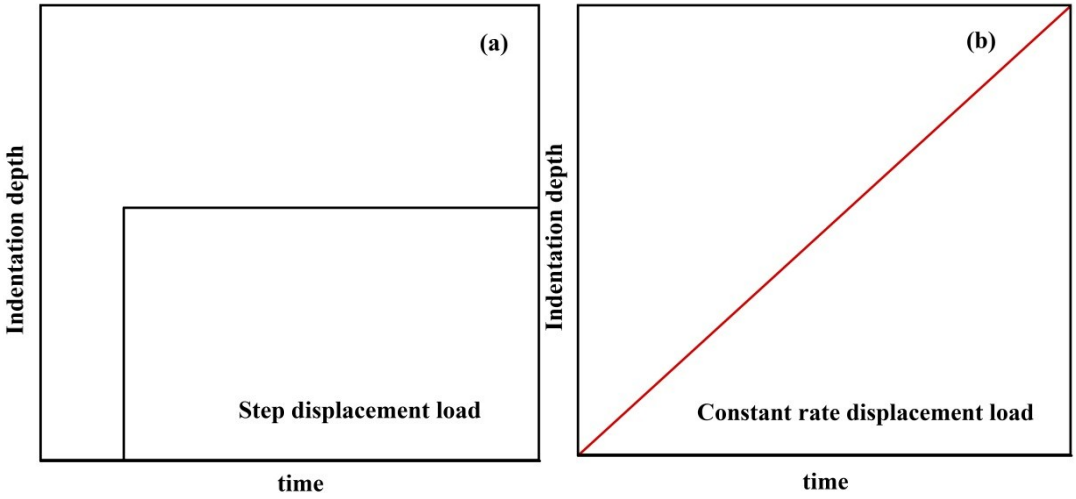

Fig. S5 The loading mode used in simulations and experiments. (a) the step displacement load; (b) the constant rate displacement load.

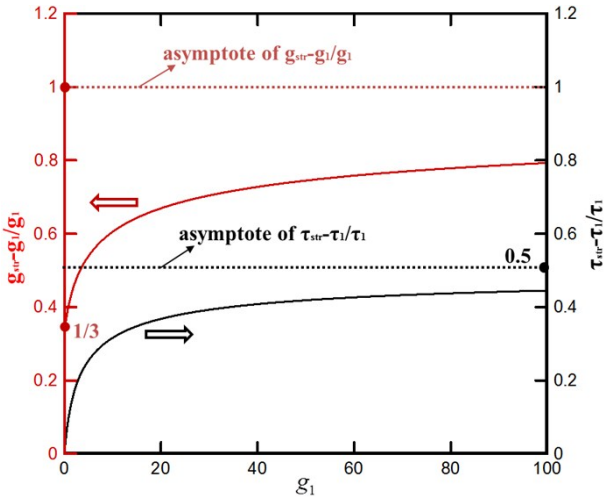

Fig. S6 The graph of $(g_{str} - g_1)/g_1$ and $(\tau_{str} - \tau_1)/\tau_1$ changing with g_1.

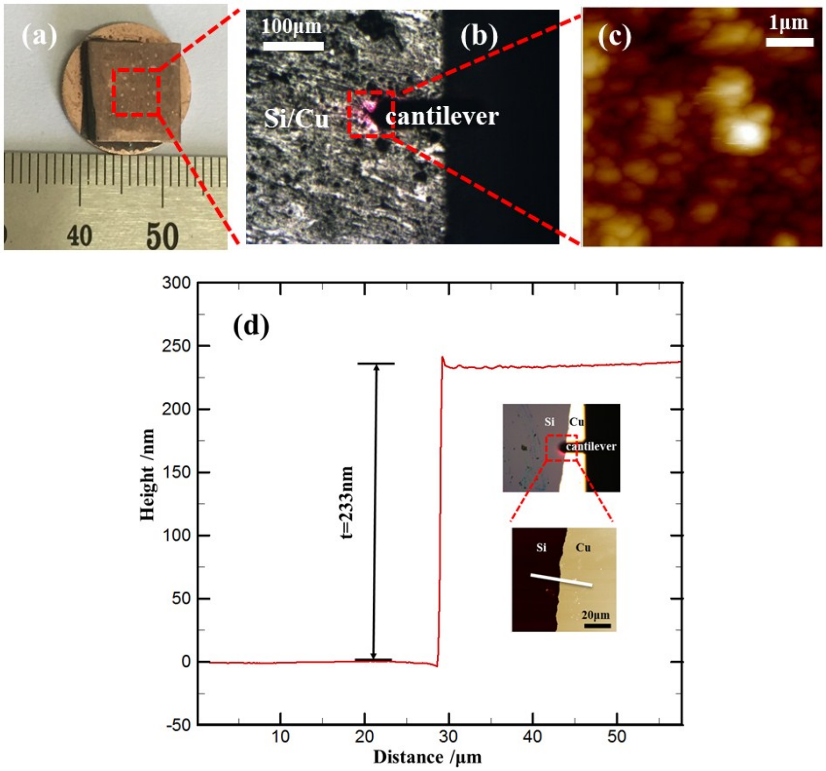

Fig. S7 The samples used in the experiments and the thickness of the Cu mounted on MVSR. (a) Photo of the Cu/MVSR; (b) Optical image of the central region of the photo of the Cu/MVSR; (c) AFM image of the central region of the optical images of the Cu/MVSR; (d) the measurement results of the copper film thickness mounted on the MVSR.

The method for measuring the copper film thickness is described as follow: While copper is plated to the top of the MVSR using an ion sputtering apparatus, a half-covered silicon wafer was placed in the ion sputtering apparatus. After that the

thickness of the copper nano film resting on the top of the silicon wafer is measured using AFM. We consider this measured value as the thickness of the copper nano film resting on the top of the MVSR.

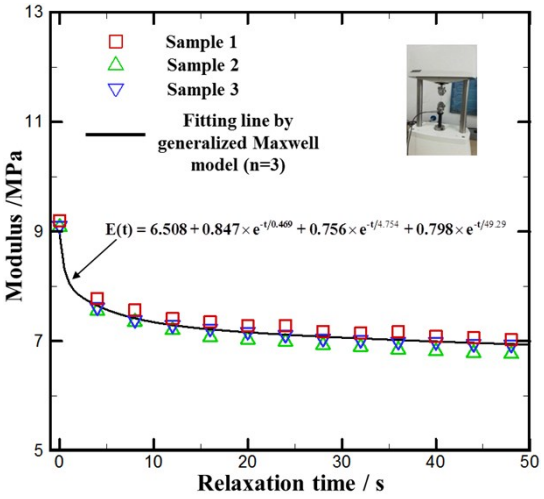

Fig. S8 the measurement results of the mechanical properties of the MVSR used in the experiments.

3.The solution process for Eqs. (21) and (22)

(1) The solution process for Eq. (21)

Before solving the relaxation time of the entire hard film/soft substrate system, the definition of relaxation time is briefly described as follows. As shown in Fig. S9, the relaxation time is the abscissa value of the intersection of the tangent line of the relaxation curve when t is zero and the line of $P = P_\infty$. For example, the relationship between the load and time of a semi-infinite three-parameter linear viscoelastic body under a step load with a spherical indenter can be described by $P(t) = \frac{4w^{3/2}R_t^{1/2}}{3}(E_1 + E_2 e^{-t/\tau})$. Then the tangent line of the relaxation curve when t is zero reads $P - \frac{4w^{3/2}R_t^{1/2}}{3}(E_1 + E_2) = -\frac{1}{\tau}\frac{4w^{3/2}R_t^{1/2}}{3}E_2 t$. In addition, $P(\infty)$ is $P(\infty) = \frac{4w^{3/2}R_t^{1/2}}{3}E_1$. Then we can know the abscissa value of the intersection of the tangent line and the line $P(\infty) = \frac{4w^{3/2}R_t^{1/2}}{3}E_1$ is τ.

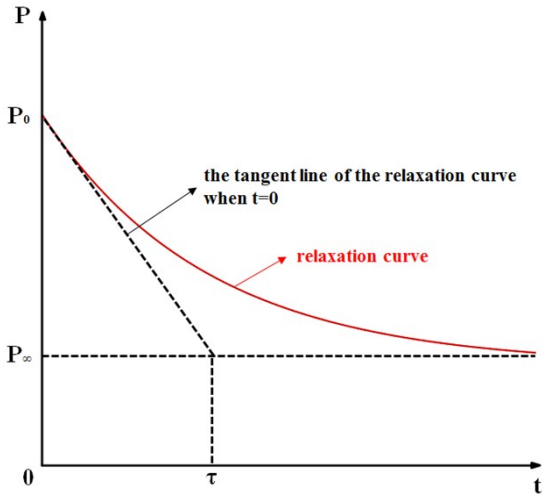

Fig. S9 the relationship between the indentation load and time under a step displacement load.

According to the definition of relaxation time, first of all, we should solve the slope of the tangent line of relaxation curve when the time equal to zero. Based on Eq. (20), we can get the slope of the tangent is

$$Q^{'}(0) = -I_2^{-1}\frac{2}{3}D^{1/3}\omega_0[\frac{E_\infty + E_1}{2(1-\nu_s^{\,2})}]^{-1/3}\frac{E_1}{2(1-\nu_s^{\,2})}\frac{1}{\tau_1} \tag{S11}$$

Then the equation of the tangent line reads:

$$Q - I_2^{-1}D^{1/3}\omega_0[\frac{E_\infty + E_1}{2(1-\nu_s^{\,2})}]^{2/3} = -I_2^{-1}\frac{2}{3}D^{1/3}\omega_0[\frac{E_\infty + E_1}{2(1-\nu_s^{\,2})}]^{-1/3}\frac{E_1}{2(1-\nu_s^{\,2})}\frac{1}{\tau_1}t \tag{S12}$$

At the same time, from Eq. (20) we can know the equilibrium indentation load is

$$Q(+\infty) = I_2^{-1}D^{1/3}\omega_0[\frac{E_\infty}{2(1-\nu_s^{\,2})}]^{2/3} \tag{S13}$$

Then, taking the Eq. (S13) into the Eq. (S12), Eq. (S12) can be expressed as

$$I_2^{-1}D^{1/3}\omega_0\frac{E_\infty^{\,2/3} - (E_\infty + E_1)^{2/3}}{[2(1-\nu_s^{\,2})]^{2/3}} = -I_2^{-1}\frac{2}{3}D^{1/3}\omega_0[\frac{E_\infty + E_1}{2(1-\nu_s^{\,2})}]^{-1/3}\frac{E_1}{2(1-\nu_s^{\,2})}\frac{1}{\tau_1}t \tag{S14}$$

Solving Eq. (S14), we can get the relaxation time of the structure:

$$t = \frac{3}{2}\tau_1[(\frac{1}{g_1}+1) - (\frac{1}{g_1})^{2/3}(\frac{1}{g_1}+1)^{1/3}] \tag{S15}$$

(2) The solution process for Eq. (22)

From Eq. (20), we can know the indentation load at the time equals to zero:

$$Q(0) = I_2^{-1} D^{1/3} \omega_0 H(t) [\frac{E_\infty + E_1}{2(1-\nu_s^2)}]^{2/3} \tag{S16}$$

Considering the structure as a material, we can know that the relationship between load and modulus should be linear according the traditional indentation model. So, based on Eq. (S16), the instantaneous modulus of the structure can be obtained:

$$E_{str}(0) = (E_\infty + E_1)^{2/3} \tag{S17}$$

At the same time, from Eq. (S13), we can get the equilibrium modulus of the structure:

$$E_{str}(\infty) = E_\infty^{2/3} \tag{S18}$$

Then, based on Eqs. (S17) and (S18), the ratio of the delay modulus to equilibrium modulus of the structure can be expressed as

$$g_{str} = \frac{E_{str-1}}{E_{str-\infty}} = \frac{(E_\infty + E_1)^{2/3} - E_\infty^{2/3}}{E_\infty^{2/3}} = (1+g_1)^{2/3} - 1 \tag{S19}$$

It should be emphasized that Eqs. (S15) and (S19) are only applicable to the hard film/soft viscoelastic substrate system with a large modulus ratio and not to the pure substrate. The reason for this is that Eqs. (S15) and (S19) are based on Eq. (20), and Eq.(20) applies only to hard film/soft viscoelastic substrate systems.